

Numerical Investigation of Transverse Wave Structures in Two-Dimensional H₂-O₂-Diluent Detonations

K. Inaba* and A. Matsuo†

Department of Mechanical Engineering, Keio University, Yokohama 223-8522, JAPAN

*Graduate Student, e-mail: m991809@msr.st.keio.ac.jp

†Assistant Professor, e-mail: matsuo@mech.keio.ac.jp

K. Tanaka‡

National Institute of Advanced Industrial Science and Technology, Tsukuba 305-8565, JAPAN

‡e-mail: tanaka-katsumi@aist.go.jp

Introduction

We usually observe an ordinary detonation in a rectangular tube. The ordinary detonation has two Mach configurations near the detonation fronts: a single Mach structure (Fig. 1a) and a double Mach structure (Fig. 1b)^{1, 2}. On the other hand, a marginal detonation occurs in a system near the detonation limit, so that it would fail if the pressure were a little lower or the channel depth a little narrower. The frontal structure of the marginal detonation is clarified³⁻⁵, and there are three Mach configurations on the transverse wave structure: the single, the double, and a complex Mach structure. In the complex Mach structure (Fig. 1c), the small front piece of the transverse wave is the reflected shock, though most of it is a transverse detonation. Strehlow and Biller⁶ define the transverse wave strength S to evaluate the transverse wave that plays an important role to the detonation propagation. With pressures of P_1 and P_3 (shown in Fig 1), the transverse wave strength S is defined as $S = P_1/P_3 - 1$. Previous studies^{6, 7} reported that in the ordinary detonation, the transverse wave strength equals to 0.5, and in the marginal detonation, 1.5. In the work of Takai et al.⁸, the relation between the post-shock conditions and the second explosion limit was experimentally investigated and they suggested that the second explosion limit might be associated with the irregularity of the H₂-Air detonations.

In the present study, two-dimensional propagating detonations are simulated in the stoichiometric hydrogen-oxygen mixtures diluted with nitrogen or argon. We treat initial pressures and inert diluents as parameters, and measure the transverse wave strengths as a function of the channel width. Through our computations, we observe flow features around the detonation fronts and detonation cell structures. The lowest post-shock conditions are determined through the cell and are utilized for the validation of the work of Takai et al.

Physical Model and Numerical Setup

The governing equations are the two-dimensional Euler equations for a chemically reacting gas system. In the current study, a 9-species, 19-reaction mechanism for **Hydrogen-Oxygen**⁹ is used. The algorithm used for solving these equations is Yee's non-MUSCL type TVD upwind explicit scheme¹⁰. The equations are integrated explicitly and the chemical reaction source term is treated in a linearly point-implicit manner. The detonable mixtures are homogeneous stoichiometric hydrogen-oxygen mixtures diluted with nitrogen or argon at initial conditions listed in Table 1. The half-reaction length in Table 1, $L_{1/2}$, is defined as the distance behind the shock at which the mass fraction of hydrogen is equal to the average of the free stream value and the equilibrium steady state value. The computations are performed with a constant grid resolution of 20.0 and 12.8 computational cells/ $L_{1/2}$ along the x and y directions, respectively. The upper and lower boundaries of the computational domain are mirror boundaries. The inflow and outflow boundaries are fixed by the unburned and burned conditions, respectively. The computation is started by mapping a one-dimensional C-J solution on a two-dimensional grid. An unburned gas pocket is placed behind the frontal shock as a trigger of the transverse wave structure. After a few thousand time-steps, well-shaped cellular structures are obtained.

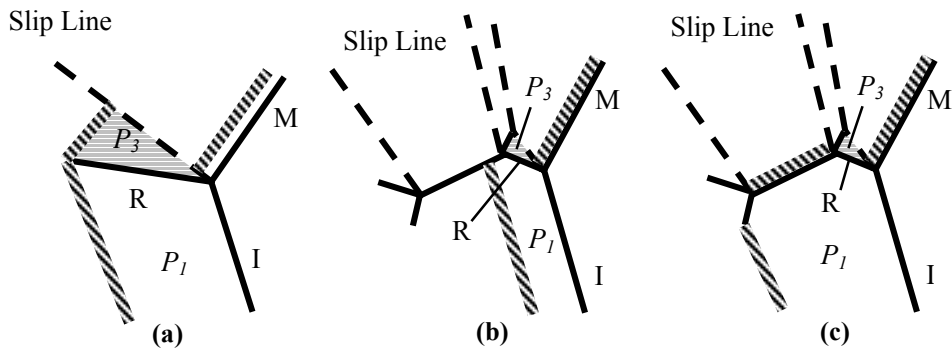


Fig. 1. Shock configuration of the frontal structure of the detonation: (a) a single Mach structure, (b) a double Mach structure, (c) a complex Mach structure. M: Mach stem, I: Incident shock, R: Reflect shock.

Results and Discussion

To sum up our all computations from Case *a* to Case *e*, we obtained the relation between the channel width and the transverse wave strength shown in Fig. 2. As the channel width is increased, the transverse wave strength increases while a single cell is appearing. The transverse wave strengths of Cases *a* and *b* increase up to 1.5, but the other cases do not go over 0.9. The cell number increases across the critical channel width and we defined these channel widths as W_{MAX} , depending on the initial conditions of the gas mixture.

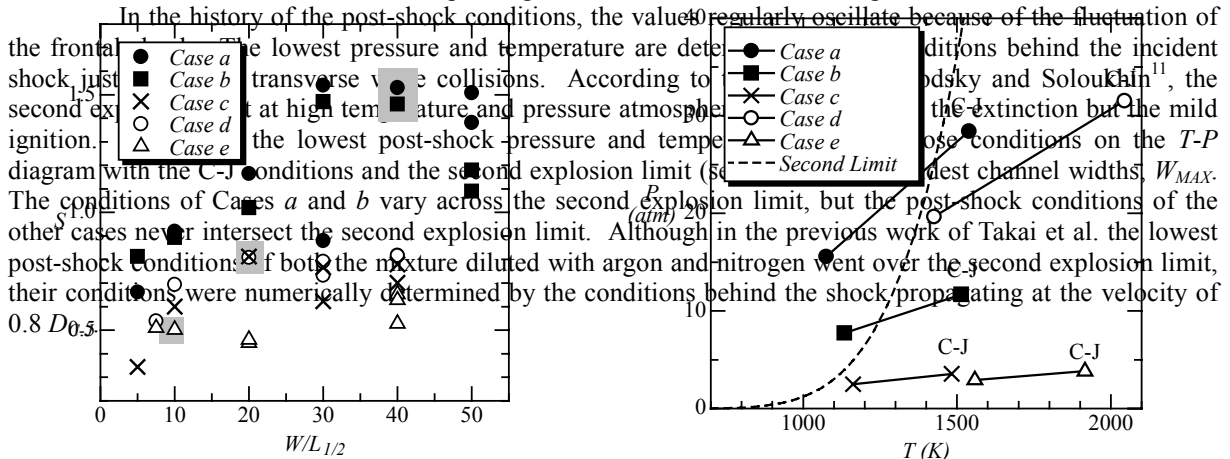


Fig. 2. Channel Width $W/L_{1/2}$ vs Transverse wave strength S (■: the widest channel width, W_{MAX}).

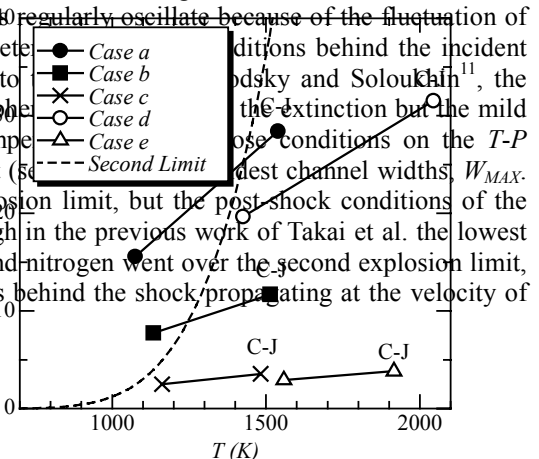


Fig. 3. T-P diagram shows post-shock conditions with the C-J conditions and the second explosion limit - Case *a*, $40L_{1/2}$; Case *b*, $40L_{1/2}$; Case *c*, $20L_{1/2}$; Case *d*, $20L_{1/2}$; Case *e*, $10L_{1/2}$ (C-J; Chapman-Jouguet detonation conditions).

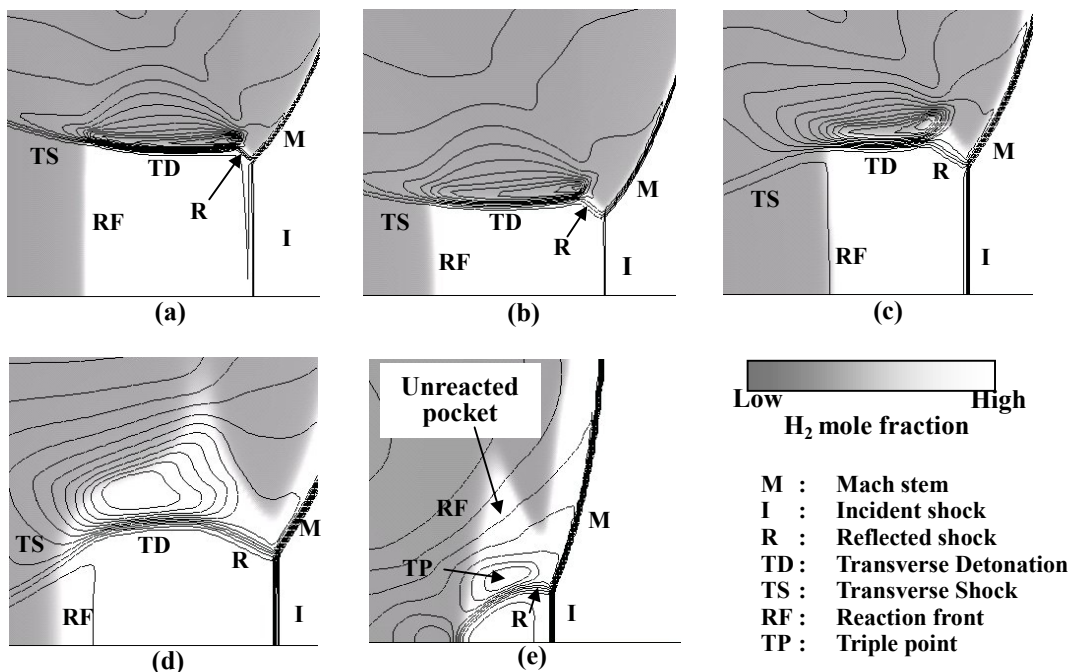


Fig. 4. Instantaneous pressure contours and mole fractions of hydrogen on background- (a) Case *a*, $W = 40L_{1/2}$, (b) Case *b*, $W = 40L_{1/2}$, (c) Case *c*, $W = 20L_{1/2}$, (d) Case *d*, $W = 20L_{1/2}$, (e) Case *e*,

Figures 4 show the pressure contours around the shock front just before the transverse wave collisions

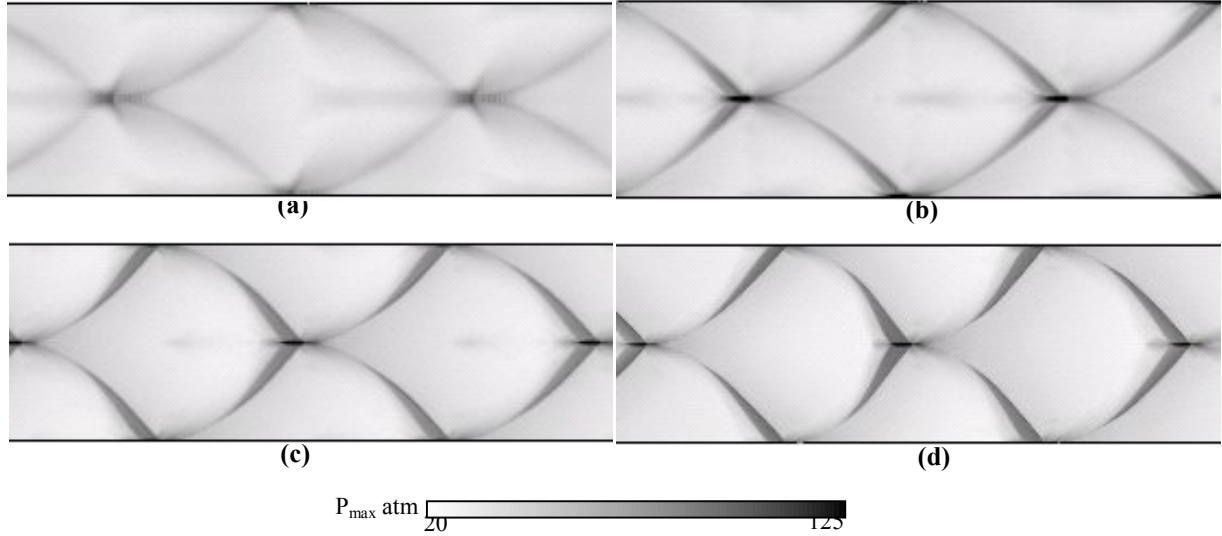


Fig. 5. Detonation histories presented by maximum pressure distributions of Case a:(a) $W = 5L_{1/2}$, 0.84mm, $a/b=1.7$, (b) $W = 10L_{1/2}$, 1.7mm, $a/b=1.6$, (c) $W = 20L_{1/2}$, 3.3mm, $a/b=1.5$, (d) $W = 40L_{1/2}$, 6.7mm, $a/b=1.4$ (W : Channel width, a/b : Aspect ratio).

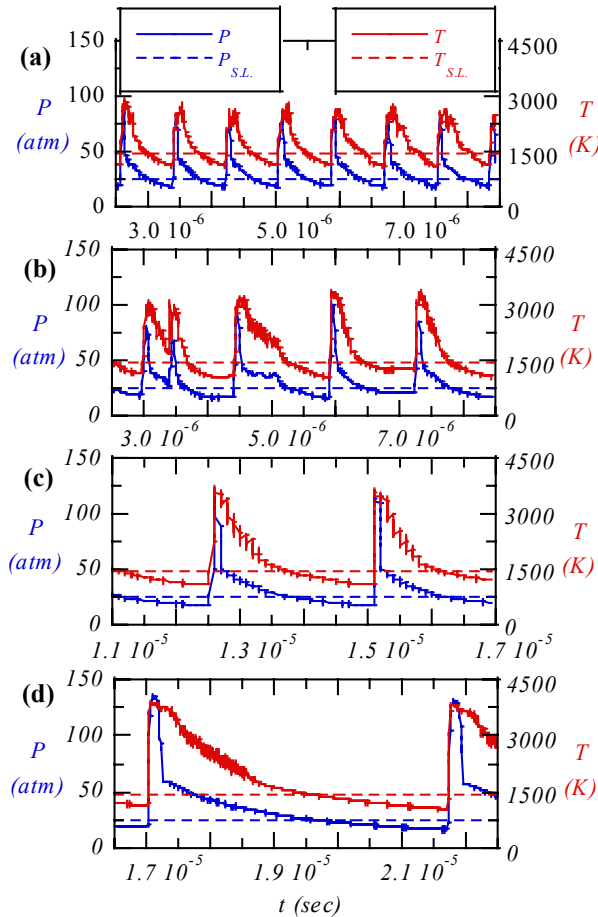


Fig. 6. Post-shock pressure and temperature histories in Case a:(a) $5L_{1/2}$, (b) $10L_{1/2}$, (c) $20L_{1/2}$, (d) $40L_{1/2}$ (Solid lines, post-shock conditions; Broken lines, the second limit).

on the background of the mole fraction of hydrogen. In Cases *a-d*, the transverse detonation occurs, and in Case *e*, an unreacted gas pocket is observed behind the shock front as shown in the hydrogen distributions. Therefore, the shock configuration of Cases *a-d* shows the complex Mach structure, and Case *e* shows the double Mach structure. Although the transverse detonation (TD) in Cases *a* and *b* precedes the transverse shock (TS) which originates from the end of the transverse detonation (Figs. 4a and 4b), the transverse detonation in Cases *c* and *d* follows the transverse shock (Figs. 4c and 4d). The preceding detonation in Cases *a* and *b* indicates that the strong transverse detonation occurs and therefore the transverse wave strengths of Cases *a* and *b* increase up to 1.5.

Let us examine the effects of the channel width on the transverse wave structures. The maximum pressure histories of the propagating detonation for different channel widths of Case *a* are shown in Fig. 5. The high-pressure regions around the triple point become gradually clearer and thicker, as the channel width increases. The aspect ratio decreases with the increase of the channel width. Owing to the occurrence of the transverse detonation, the contrast of the maximum pressures becomes clear, and the propagating velocity of the transverse waves goes up. As for the transverse wave structure, Fig. 5a - $W = 5L_{1/2}$ - corresponds to the W_{MAX} of Case *e* (the double Mach structure), and Figs. 5b and 5c - $W = 10L_{1/2}$ and $20L_{1/2}$, respectively - do to those of Cases *c* and *d* (the complex Mach structure with a normal transverse detonation). The

post-shock pressure and temperature histories on the centerline of the cell (Solid lines) are shown in Figs. 6. In these $P-t$ diagrams, all of the post-shock conditions oscillate across the conditions corresponding to the second explosion limit (Broken lines), and the lowest post-shock conditions in Figs. 6a-6c agree with those in Fig. 6d - $W = 40L_{1/2}$ - (the complex Mach structure with the strong transverse detonation). Then, it is difficult to simply say that the transverse wave structure relates to the post-shock conditions. The strong transverse detonation, however, occurs only in the case where the post-shock conditions vary across the second explosion limit. The details of the transverse wave structure remains as a matter to be examined in the future.

Summary

Two-dimensional computations of propagating detonations in stoichiometric hydrogen-oxygen mixtures diluted with nitrogen and argon were performed using a detailed chemical reaction mechanism. The transverse wave strength was defined as the dimensionless pressure increase across the reflected shock and was determined for different channel widths. The transverse waves evolved as a function of the channel width, and its strength grew up while a single cell is appearing. Although the complex Mach structure is observed except for the hydrogen-oxygen-argon mixture at initial pressure 0.132 atm, the strong transverse detonation occurs only in the hydrogen-air mixture at 1.00 and 0.421 atm. The effect of the post-shock pressure and temperature on the transverse wave structure was examined, and the possibility that the second explosion limit has an important role to the occurrence of the strong transverse was indicated.

Acknowledgements

This work was supported by the Research Fellowships of the Japan Society for the Promotion of Science for Young Scientists.

References

- [1] Gamezo, V.N., Desbordes, D., and Oran, E.S., *Shock Waves*, 9, (1999), pp. 11-17.
- [2] Gamezo, V.N., Desbordes, D., and Oran, E.S., *Combust. Flame*, 116, (1999), pp. 154-165.
- [3] Strehlow, R.A. and Crooker, A.J., *Acta. Astronautica*, 1, (1970), pp.303-315.
- [4] Lefebvre, M. H. and Oran, E. S., *Shock Waves*, 4, (1995), pp. 277-283.
- [5] Oran, E. S., Weber, JR., J. W., Stefaniw, E. I., Lefebvre, M. H., Anderson, JR., J. D., *Combust. Flame*, 113, (1998), pp. 147-163.
- [6] Strehlow, R.A. and Biller, J.R., *Combust. Flame*, 13, (1969), pp.577-582.
- [7] Edwards, D., H., Hooper, G., Job, E., M., and Parry, D., J., *Astronaut. Acta*, 15, (1970), pp. 323-333.
- [8] Takai, R., Yoneda, K., and Hikita, T., 15th Symposium (International) on Combustion, The Combustion Institute, Pittsburgh, Pa., (1974), pp. 69-78.
- [9] Wilson, G. J. and MacCormack, R. W., AIAA-90-2307, (1990).
- [10] Yee, H.C., NASA TM 89464, (1987).
- [11] Voevodsky, V. V. and Soloukhin, R. I., 10th Symposium (International) on Combustion, The Combustion Institute, Pittsburgh, Pa., (1965), pp. 279-283.